Cytotoxicity and Antibacterial Activity of Ag@MOF-5 Loaded Alginate–Gelatin Hydrogel as a Promising Antimicrobial Biomaterial

by Perpustakaan IIK Bhakti Wiyata

Advanced Journal of Chemistry, Section A, 2026, 9(4), 577-593

Advanced Journal of Chemistry, Section A

Journal homepage: www.ajchem-a.com

Original Research Article

Cytotoxicity and Antibacterial Activity of Ag@MOF-5 Loaded Alginate–Gelatin Hydrogel as a Promising Antimicrobial Biomaterial

Tri Ana Mulyati[1,*], Juni Ekowati[2], Atmira Sariwati[3], Lia Agustina[1], Fery Eko Pujiono[1]

[1]Departement of Pharmacy, Institut Ilmu Kesehatan Bhakti Wiyata, Kediri, Indonesia
[2]Departement of Pharmaceutical, Airlangga University, Surabaya, Indonesia
[3]Departement of Traditional Chinese Medicine, Institut Ilmu Kesehatan Bhakti Wiyata, Kediri, Indonesia

ARTICLEINFO

Article history

Submitted: 2025-09-16
Revised: 2025-10-22
Accepted: 2025-10-27
ID: AJCA-2509-1928
DOI: 10.48309/AJCA.2026.547525.1928

KEYWORDS

Hydrogel
MOF-5
Ag
Antibacterial
Cytotoxicity
Alginate
Gelatin

ABSTRACT

The development of safe multifunctional biomaterials that possess antibacterial activity is of great importance. In this study, a composite alginate–gelatin hydrogel incorporating silver-modified MOF-5 was developed to enhance antibacterial activity. The successful synthesis of the samples was confirmed by XRD characterization of MOF-5, showing characteristic peaks at 2θ = 6.8°, 9.6°, and 13.7°, which remained identifiable after modification with Ag. FTIR analysis of the Hy/Ag(20)@MOF-5 sample indicated an interaction between the carboxylate groups (–COO–) of alginate and the amino groups ($–NH_2$) of gelatin, with the absorption band shifting from 1583 cm^{-1} to 1545 cm^{-1}, signifying the incorporation of Ag@MOF-5 within the hydrogel matrix. SEM-EDX results of Hy/Ag(20)@MOF-5 revealed a uniformly porous surface structure and confirmed the presence of Zn, O, and Ag elements. Ag@MOF-5 in alginate-gelatin hydrogel causes a decrease in the swelling ratio and biodegradability percentage. The release profile of Ag indicates that in the Hy/Ag(20)@MOF-5 sample, the concentration of released Ag is higher at 7.4 µg/mL after 24 hours; however, the release of Ag ions remains controlled. The cytotoxicity test, shows a cell viability of over 79 % across all sample types, categorizing them as non-toxic within the tested concentration range. The antibacterial activity test results indicate that the hy/Ag(20)@MOF-5 sample exhibits the highest antibacterial activity against *Staphylococcus aureus* and *Escherichia coli*, with MIC values of 1.2 ± 0.1 and 1.0 ± 0.1 mg/mL, respectively, and MBC values of 2.5 ± 0.1 and 2.7 ± 0.2 mg/mL, and is capable of killing all bacteria within 24 hours.

GRAPHICALABSTRACT

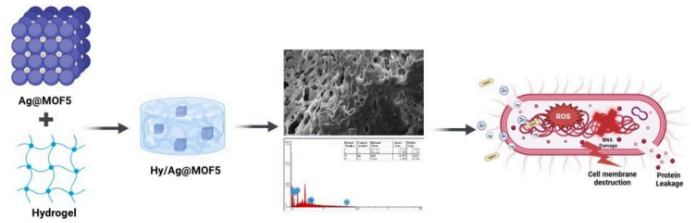

* Corresponding author: Mulyati, Tri Ana
✉ E-mail: tri.ana.mulyati@iik.ac.id

Introduction

The most commonly encountered complications of diabetes mellitus are the pathological changes in the extremities, namely, pain in the feet and the emergence of wounds (diabetic ulcers). DM patients suffering from diabetic ulcers generally experience open ulceration that is difficult to heal [1,2]. Diabetic ulcer wounds can be exacerbated by immune system disorders and bacterial resistance due to high blood glucose levels [3]. Research conducted by Mulyati *et al.* [4] indicates that in a sample of PUS patients with DM in Kediri City, 48 isolates containing various types of bacteria were found, namely *Staphylococcus aureus* (38 %), Pseudomonas aeruginosa (23.2 %), Bacillus subtilis (21 %), and *Escherichia coli* (18 %), all of which were proven to be resistant to antibiotics. One approach that can address this issue is the development of Metal Organic Frameworks (MOF).

MOF (Metal-Organic Framework) is a porous material composed of metal clusters connected by organic ligands to form a framework [5]. MOFs are extensively developed as antibacterial and wound-healing materials due to their various advantages, such as the ability to oxidize and depolarize the outer membrane of bacterial cells [6], enhancing the formation of ROS (reactive oxygen species) that can damage bacterial DNA [7]. Among the various types of MOFs, zinc-based MOFs (Zn) have garnered special attention as they exhibit significant antibacterial activity against Gram-positive and Gram-negative bacteria. A study by Mulyati *et al*. [8] reported that MOF-5 generated an inhibitory zone diameter of 38.9 ± 1 mm against *Staphylococcus aureus* and 36.2 ± 1 mm against *Escherichia coli*, indicating its potential as a broad-spectrum antimicrobial agent. One of the metal-organic frameworks (MOFs) frequently used for chronic wound healing is MOF-5, which is composed of zinc and benzendicarboxylic acid. MOF-5 offers several advantages, including a highly porous structure, excellent biocompatibility, and controlled Zn^{2+} ion release. These characteristics facilitate efficient drug loading and release as well as optimal antibacterial and regenerative effects [9,10]. Furthermore, compared to other MOFs (based on Cu, Ag, or Fe), MOF-5 has the advantage of lower cytotoxicity risk and more stable degradation in biological environments. The released Zn^{2+} ions not only inhibit bacterial growth but also enhance angiogenesis, fibroblast proliferation and collagen synthesis, all of which are crucial for the healing of chronic wounds such as diabetic ulcers [9,11].

MOFs are known to have higher persistence than conventional antibiotics and exhibit synergistic effects when modified with other bioactive compounds. Research by Shakya [12] demonstrated that silver-modified Co-MOF (HKUST-1) could reduce the populations of *E. coli* and *S. aureus* by up to 90 %, reinforcing silver-modified MOFs' role in antimicrobial therapy applications. Although silver-modified MOFs exhibit very strong antibacterial activity, the topical application of MOFs on wounds faces numerous challenges, such as potential particle aggregation, low adhesion to wound tissue, and the risk of local toxicity [13]. Modification of MOF-5 with AgNPs results in a synergistic antibacterial effect, where Zn^{2+} ions from MOF-5 act as bacteriostatic agents by disrupting cell membranes and metabolic enzymes, while Ag^{+} ions are bactericidal, damaging bacterial DNA and proteins [14,15]. The combination of both provides a broad-spectrum antibacterial activity and high killing efficiency. Additionally, the porous structure of MOF-5 serves as a carrier and controlled release platform for AgNPs, preventing the toxic spikes that typically occur with direct use of AgNPs [15]. Several approaches can be taken to address these issues, including developing MOFs in hydrogel preparations.

Hydrogel is a formulation that has a porous structure capable of absorbing wound fluids and has the advantage of being easily modified

without changing its fundamental properties [16]. Research by Vincekovic *et al*. [17] also shows that composite alginate/gelatin/AgNPs hydrogels can enhance antibacterial activity up to 85 %. Alginate and gelatin-based composite hydrogels have a porous structure suitable for addressing moist and purulent wounds such as burns and diabetic ulcers [18]. This finding is supported by Maghsoudi *et al.* [19], who reported the antibacterial effectiveness of alginate-gelatin hydrogels containing Zn-MOF (MOF-8) reaching 99 % against *E. coli* and *S. aureus*. On the other hand, research on the modification of Ag in MOF-5 and its formulation in alginate-gelatin-based hydrogels is still limited, especially for multi-resistant antibacterial applications. Therefore, in this study, alginate-gelatin hydrogel containing Ag@MOF-5 will be developed, and its cytotoxicity and antibacterial activity will be evaluated as an effective antibacterial hydrogel.

Experimental

Materials

The materials used in this study are Zinc (II) nitrate hexahydrate ($Zn(NO_3)_2•6H_2O$), terephthalic acid (H_2BDC), and Potassium chloride (KCl) with a purity of 99.0 % supplied by Sigma-Aldrich, chloroform ($CHCl_3$), methanol (CH_3OH), N,N-dimethylformamide (DMF), sodium alginate (medium viscosity), gelatin from porcine skin (Type A, Bloom 300), silver nitrate ($AgNO_3$), phosphate-buffered saline (PBS, pH 7.4), nitric acid (HNO_3, 65 %), dimethyl sulfoxide (DMSO), and 3-(4,5-dimethylthiazol-2-yl)-2,5-diphenyltetrazolium bromide (MTT), Luria Bertani (LB), and Nutrient Agar (NA), with a purity of 99.0 % supplied by Merck. The test bacterial strains used were *Staphylococcus aureus* ATCC 33591 (gram-positive) and *Escherichia coli* ATCC 25922 (gram-negative), obtained from the Yogyakarta Health Laboratory Center. At the same time, Baby Hamster Kidney cells (BHK-21, CCL-10) were supplied by the Institute of Tropical Disease – Airlangga University, Surabaya. Minimum Essential Medium Eagle (MEM, Gibco, Thermo Fisher Scientific, USA) supplemented with 10 % fetal bovine serum (FBS), penicillin (100 U/mL), and streptomycin (100 µg/mL) was utilized for cell culture.

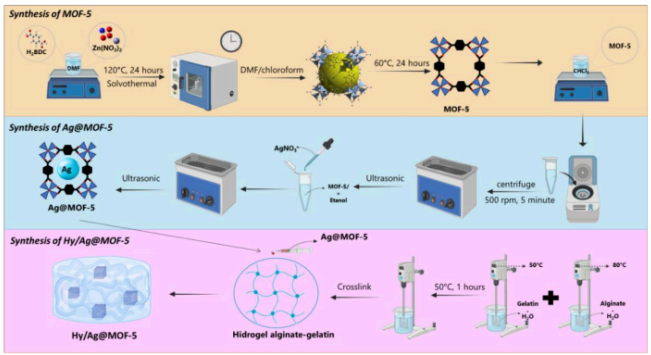

Figure 1. Schematic representation of the synthesis of alginate–gelatin composite hydrogel modified with Ag@MOF-5.

Methods

Formation of algin-gelatin composite hydrogel modified Ag@MOF-5

The formation of the alginate-gelatin composite hydrogel modified Ag@MOF-5 begins with the synthesis of MOF-5 via the solvothermal method, followed by the modification of MOF-5 with silver ($AgNO_3$) through an ultrasonic method. The synthesis is performed by integrating Ag@MOF-5 into the alginate-gelatin hydrogel matrix, resulting in the composite Hy/Ag@MOF-5. Below is the procedure for each stage of the formation of Hy/Ag@MOF-5. Figure 1 illustrates the alginate-gelatin composite hydrogel modified Ag@MOF-5 synthesis process.

Synthesis of MOF-5

The first stage of the synthesis of MOF-5, represented as *Step I* in Figure 1, involves the preparation of MOF-5 following the modified methods of Ediati *et al.* [5] and Hu *et al.* [20]. Initially, $Zn(NO_3)_2{\bullet}6H_2O$ and terephthalic acid (H_2BDC) were reacted in a molar ratio 3:1 in 60 mL of DMF. The mixture was stirred with a magnetic stirrer for 30 minutes until homogeneous. The solution was then transferred to a Teflon container and heated in an oven at 120 °C for 24 hours without stirring (static). The resulting precipitate was subsequently washed with DMF and chloroform three times. The solid was then dried under vacuum at 60 °C and named MOF-5.

Synthesis of Ag@MOF-5

MOF-5 with silver was modified by modifying the method of Mulyati *et al.* [8] and Sacourbaravi *et al.* [28] as shown in *Step II* of Figure 1. Initially, 1 gram of MOF-5 powder was dispersed in 10 mL of chloroform for 5 days. The suspension was then centrifuged at 500 rpm for 5 minutes. The resulting solid was subsequently dried at 80 °C for 24 hours. The solid was then weighed at 0.1 grams and added to 10 mL of $AgNO_3$ solution with concentrations of 10 mg/mL and 20 mg/mL. The solutions were reacted under ultrasonic conditions for 10 minutes. The final solid was filtered and tested for free silver ions using a KCl solution. The solid was subsequently dried under vacuum at 60 °C and designated as Ag(10)@MOF-5 and Ag(20)@MOF-5.

Synthesis of Hy/Ag@MOF-5

The synthesis of composite alginate-gelatin hydrogel modified with Ag@MOF-5 was performed by modifying the research of Maghsoudi *et al.* [19] as shown in *Step III* of Figure 1. Initially, sodium alginate and gelatin were dissolved in distilled water at 12 % w/v and 6 % w/v, respectively. The sodium alginate solution was heated while stirring at 80 °C, while the gelatin solution was heated at a temperature of 50 °C for 1 hour until fully dissolved. Both solutions were mixed in a 1:1 ratio and then stirred again at 50 °C until a homogeneous polymer mixture was formed, which is referred to as Hy. The resulting alginate-gelatin hydrogel (Hy) was then supplemented with solid MOF-5, Ag(10)@MOF-5, and Ag(20)@MOF-5, each at a concentration of 10 % w/v and 20 % w/v. The mixing was conducted using a sterile syringe. The mixture was centrifuged at a speed of 1000 rpm for 1 minute. The modified alginate-gelatin hydrogel is subsequently referred to as Hy/MOF-5, Hy/Ag(10)@MOF-5, and Hy/Ag(20)@MOF-5.

Characterization

Material characterization is utilized to confirm the formation of MOF-5, Ag@MOF-5, and modified alginate-gelatin hydrogel Ag@MOF-5, referring to the studies by Xiong *et al.* [22], Mulyati *et al.* [8], and Maghsoudi *et al.* [19] employing X-ray Diffraction (XRD), Attenuated Total Reflectance – Fourier Transform Infrared Spectroscopy (ATR-

FTIR), Scanning Electron Microscopy (SEM), Energy Dispersive X-ray Spectroscopy (EDS), and Thermogravimetric Analysis (TGA). The diffractogram patterns of MOF-5 and Ag@MOF-5 were analyzed using a JEOL diffractometer (Cu Kα radiation, λ = 1.54056 Å, 40 kV, 30 mA) over the range of 2θ 5–50 °. This analysis was conducted to identify the characteristic crystal peaks of MOF-5 and its changes upon modification with silver ($AgNO_3$). The thermal stability of MOF-5 and Ag@MOF-5 was assessed through TGA analysis (Mettler Toledo) in the temperature range of 30–600 °C with a heating rate of 10 °C/min in a nitrogen atmosphere, resulting in a thermal degradation profile. The analysis of functional groups was conducted on MOF-5, Ag@MOF-5, Hy, Hy/MOF-5, Hy/Ag(10)@MOF-5, and Hy/Ag(20)@MOF-5 using ATR-FTIR (Shimadzu Corporation, Japan) at wavenumbers ranging from 400 to 4000 cm^{-1}. This analysis was employed to identify the functional groups of the samples and the chemical interactions between the hydrogel and Ag@MOF. Surface morphology analysis was performed on MOF-5, Ag@MOF-5, Hy, Hy/MOF-5, Hy/Ag(10)@MOF-5, and Hy/Ag(20)@MOF-5 using SEM (Zeiss EVO MA10) with a gold coating (Au coating). The success of silver modification is demonstrated through elemental analysis with EDS on Hy/Ag@MOF-5 to verify the presence of silver elements within the alginate-gelatin hydrogel matrix.

Swelling test

The swelling test was conducted to evaluate the fluid absorption capacity of the samples Hy, Hy/MOF-5, Hy/Ag(10)@MOF-5, and Hy/Ag(20)@MOF-5 according to the procedure by Maghsoudi *et al*. [19]. Each sample was weighed at 1 gram at a constant weight at 37 °C and recorded as W_0. Each sample was immersed in 3 mL of phosphate-buffered saline (PBS, pH 7.4) at 37 °C. At 30, 60, 120, 180, 240, 300, and 360 minutes, the samples were removed and weighed again as W_t. The swelling ratio was calculated using the Equation 1:

$$\text{Swelling Ratio} = \frac{W_t - W_0}{W_0} \quad (1)$$

Biodegradation test

The biodegradation test was conducted to determine the stability of samples Hy, Hy/MOF-5, Hy/Ag(10)@MOF-5, and Hy/Ag(20)@MOF-5 in a physiological medium according to the procedure by Maghsoudi *et al.* [19]. Each sample was weighed at 1 gram to achieve a constant weight at a temperature of 37 °C and recorded as W_0. Each sample was immersed in 3 mL of phosphate-buffered saline (PBS, pH 7.4) at 37 °C. The samples were dried at 5, 10, 15, 20, 25, and 27 days until a constant weight was achieved and recorded as W_t. The percentage of degradation at a specific time was calculated using the Equation 2:

$$\text{Degradation (\%)} = \frac{W_0 - W_t}{W_0} \times 100\ \% \quad (2)$$

Ag release test

The Ag release test is conducted to determine the Ag release profile from the Hy/Ag(10)@MOF-5 and Hy/Ag(20)@MOF-5 samples using modified procedures from Xiong *et al.* [22] and Far *et al.* [23]. Each sample is weighed at 1 gram and then submerged in 10 mL of phosphate-buffered saline (PBS, pH 7.4) at a temperature of 37 °C. At time intervals of 0, 6, 12, and 24 hours, the entire soaking solution is collected and nitric acid (HNO_3, 2 % v/v) is added to fully dissolve the Ag^+ ions before analysis using Inductively Coupled Plasma–Optical Emission Spectroscopy (ICP–OES).

Cytotoxicity test (MTT Assay)

The cytotoxicity test was conducted using the MTT Assay method on BHK-21 (Baby Hamster Kidney) cells cultured in MEM Eagle medium. This cytotoxicity test was performed by modifying the research of Urzedo *et al*. [24]. BHK-21 cells were

maintained in an incubator at 37 °C with a 5 % CO_2 atmosphere. BHK-21 cells were seeded in a 96-well plate at a density of 1.5 × 10^4 cells/well in a volume of 100 µL, and then incubated for 24 hours until they reached approximately 80 % confluence. Each sample, namely Hy, Hy/MOF-5, Hy/Ag(10)@MOF-5, and Hy/Ag(20)@MOF-5, was extracted in the culture medium at 37 °C for 24 hours. The culture medium was then replaced with hydrogel elution medium at various concentrations (1, 2, 4, 8, and 15 µg/mL) and incubated for 24 hours under the same conditions. After incubation, 5 mg/mL MTT solution was added to each well and incubated for 3–4 hours until formazan crystals formed. The formed formazan crystals are subsequently dissolved in 100 µL of DMSO. Absorbance is measured using an ELISA reader at a wavelength of 570 nm. The percentage of cell viability is calculated by comparing the absorbance values of the samples to the negative control. All experiments were performed in triplicate (n = 3), and the results were expressed as mean ± standard deviation (SD) to ensure data reliability. The assay was intended to evaluate cytotoxic behavior qualitatively based on the cell viability threshold (≥ 70 % indicates non-toxic).

Antibacterial activity

The antibacterial activity of the samples Hy, Hy/MOF-5, Hy/Ag(10)@MOF-5, and Hy/Ag(20)@MOF-5 was tested against the Gram-positive bacterium *Staphylococcus aureus* (ATCC33591) and the Gram-negative bacterium *Escherichia coli* (ATCC25922). The determination of the Minimum Inhibitory Concentration (MIC) and Minimum Bactericidal Concentration (MBC) was conducted using the broth microdilution method according to the procedures of Li *et al.* [25]. A standard bacterial suspension of 1 × 10^6 CFU/mL was inoculated into microplates containing the samples in nutrient broth media. Each well was incubated at 37 °C for 24 hours. The MIC was established as the lowest concentration of the hydrogel extract, and it showed no bacterial growth. For the MBC determination, aliquots from wells that showed no bacterial growth were inoculated onto nutrient agar media and incubated at 37 °C for 24 hours. The lowest concentration that does not produce colony growth, or that reduces the number of colonies by ≥ 99.9 %, is expressed as MBC. The bacterial growth kinetics test is also conducted according to the method of Maghsoudi *et al.* [19]. Samples are incubated with bacterial suspension (1 × 10^6 CFU/mL) at a temperature of 37 °C. At specific time intervals of 3, 6, 12, and 24 hours, aliquots are taken and serially diluted. The samples are then plated on nutrient agar media and incubated at 37 °C for 24 hours. The number of colonies (CFU/mL) formed is counted to evaluate the bactericidal effects of the samples. All antibacterial experiments (MIC, MBC, and growth kinetics) were performed in triplicate (n = 3). The MIC and MBC data were expressed as mean ± SD. Normality and homogeneity of variance were verified using the Shapiro–Wilk and Levene's tests. One-way ANOVA followed by Tukey's post hoc test was applied to determine significant differences among groups, with $p < 0.05$ considered statistically significant. Statistical analyses were performed using SPSS version 21 (IBM, USA).

Results and Discussion

In this study, the synthesis of alginate-gelatin Hy/Ag@MOF-5 has been successfully conducted. Initially, the white solid MOF-5 was successfully synthesized through a solvothermal reaction between $Zn(NO_3)_2$•$6H_2O$ and terephthalic acid (H_2BDC) in DMF [20]. The modification of MOF-5 with $AgNO_3$ at concentrations of 10 mg/mL and 20 mg/mL resulted in brownish solids, indicating the initial successful incorporation of Ag ions into the MOF-5 framework, subsequently referred to as Ag(10)@MOF-5 and Ag(20)@MOF-5. This color

change phenomenon showed that the modification of Ag ions within the MOF framework alters the electronic structure and light emission absorption, thereby affecting the optical properties of the solid [26]. The alginate-gelatin hydrogel was also successfully synthesized by mixing sodium alginate (12 %b/v) and gelatin (6 %b/v) solutions in a 1:1 ratio, subsequently referred to as Hy. This ratio was selected because it produces a hydrogel with a sufficiently dense yet elastic consistency, facilitating the integration of active materials. The stability of this hydrogel is supported by intermolecular interactions between the carboxylate groups in alginate and the amine groups in gelatin through hydrogen bonding and electrostatic interactions, which play a crucial role in forming the gel consistency [27].

Samples of Hy and Hy/MOF-5, exhibit a milky white color and a smooth texture. The integration of Ag@MOF-5 into the hydrogel produces a noticeable visual change, transitioning to a brownish hue in both Hy/Ag(10)@MOF-5 and Hy/Ag(20)@MOF-5 samples, reflecting the presence of Ag@MOF-5 particles within the alginate-gelatin hydrogel. This color change indicates a successful modification of the hydrogel with Ag@MOF-5 and serves as an initial indication of particle distribution within the gel matrix [28]. The samples Hy/Ag(10)@MOF-5 and Hy/Ag(20)@MOF-5 also exhibit the presence of non-homogeneous solids within the hydrogel matrix. This phenomenon is attributed to the mixing of MOF in the hydrogel, which often results in weak interactions between MOF particles and the polymer matrix, leading to agglomeration and uneven distribution [29]. These findings highlight the need for the development of synthesis methods for the alginate-gelatin/Ag@MOF-5 composite hydrogel to address this issue.

The crystallinity of the MOF-5 and Ag@MOF-5 samples was analyzed using Powder X-Ray Diffraction (PXRD), and the recorded patterns are illustrated in Figure 2. The XRD analysis shows that there are characteristic peaks of MOF-5 at 2θ = 6.8 °; 9.6 °; 13.7 °; 15.5 °; 19.3 °; 20.7 °; 22.5 °; 31.7 °; 36.3 °; and 42.5 ° [8,20]. Meanwhile, Ag@MOF still retains the characteristic pattern of MOF-5 but exhibits distinct peaks at 9 ° and 45 ° [20,30]. The difference between Ag(10)@MOF-5 and Ag(20)@MOF-5 is observed in the characteristic peaks at 9 ° and 45 °, where the higher the Ag concentration, the greater the intensity of the pattern.

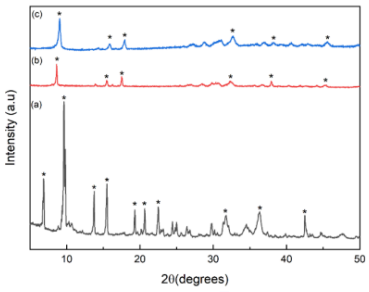

Figure 2. PXRD patterns of (a) MOF-5; (b) Ag(10)@MOF-5; (c) Ag(20)@MOF-5.

Hy/Ag@MOF is confirmed by comparing the FTIR spectra of MOF-5, Ag@MOF-5, Hy, Hy/Ag(10)@MOF-5, and Hy/Ag(20)@MOF-5 as presented in Figure 3. The FTIR spectrum of MOF-5 exhibits characteristic peaks such as O-H, C=O, C-O, C-O-C, and ZnO at 3180 cm^{-1}, 1583 cm^{-1}, 1545 cm^{-1}, 1498 cm^{-1}, 1019 cm^{-1}, and 595 cm^{-1}, respectively[8]. On the other hand, the Ag@MOF-5 spectrum shows the characteristic peaks of MOF-5 namely O-H, C=O, C-O, C-O-C, and ZnO at 3194 cm^{-1}, 1501 cm^{-1}, 1017 cm^{-1}, and 647 cm^{-1} [31,32]. The difference between MOF-5 and Ag@MOF-5 is noted in the C=O peak, where MOF-5 displays a double peak, while Ag@MOF-5 shows a single peak, indicating the interaction between MOF-5 and nano Ag.

The thermal decomposition behavior of MOF-5 and Ag@MOF-5 is illustrated in Figure 4, which

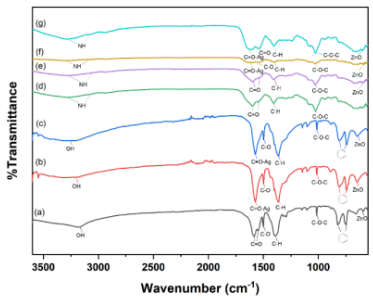

Figure 3. FTIR spectra of (a) MOF-5; (b) Ag (10) @MOF-5; (c) Ag (20) @MOF-5; (d)Hy; (e) Hy/MOF-5; (f) Hy/Ag (10) @MOF-5; (g) Hy/Ag (20) @MOF-5.

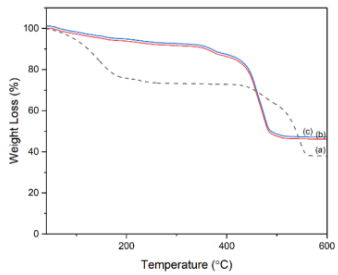

Figure 4. TGA curves of (a) MOF-5; (b) Ag (10) @MOF-5; (c) Ag (20) @MOF-5.

demonstrates that the TGA curve of mass loss for MOF-5 is observed over a wide temperature range up to 600 °C. The initial loss is observed up to a temperature of 180 °C, attributed to the decomposition of the 1,4-benzenedicarboxylate framework. Subsequently, a relatively slow mass loss occurs with increasing temperature. A significant mass loss occurs between 400 °C and 600 °C, amounting to 32.3 %, indicating that the entire MOF structure has deteriorated, leaving only ZnO residue [33,34]. At 600 °C, 37.8 % of MOF-5 remains, which signifies its thermal stability. On the other hand, Ag@MOF-5 displays an initial mass loss which differs from MOF-5, occurring at a temperature of 400 °C due to the interaction between Ag and MOF. This interaction binds the ligands more strongly and renders the MOF framework more rigid [35,36]. The decrease recorded is the highest at 46.2 %, indicating the degradation of the MOF structure. At temperatures ranging from 486 °C to 600 °C, Ag@MOF-5 remains at 45.8 %. Furthermore, the difference between Ag (10) @MOF-5 and Ag (20) @MOF-5 lies in the remaining amounts at 486 °C to 600 °C, where Ag (10) @MOF-5 remains at 45.8 %, while Ag (20) @MOF-5 remains at 50.2 %.

The surface morphology and elements of MOF-5, Ag@MOF-5, Hy, Hy/MOF-5, and Hy/Ag@MOF-5 has been analyzed using Scanning Electron Microscopy and Energy Dispersive X-ray Spectroscopy (SEM-EDS) as shown in the Figure 5. The Figures indicate that MOF-5 has a regular cubic shape [5,8], while Ag@MOF-5 exhibits a flake-like shape with a rough surface due to the presence of Ag nanoparticles [30,37]. Hy shows an irregular porous shape and smooth texture. Furthermore, after the addition of MOF-5, Hy/MOF-5 retains a smooth form, and the pores of the Hydrogel become closed. On the other hand, Hy/Ag@MOF-5 exhibits open, regular, and smaller pores compared to the original Hydrogel, which indicates the formation of Hydrogel modified with Ag@MOF-5. The results are also supported by the EDS findings, as shown in Figure 5.

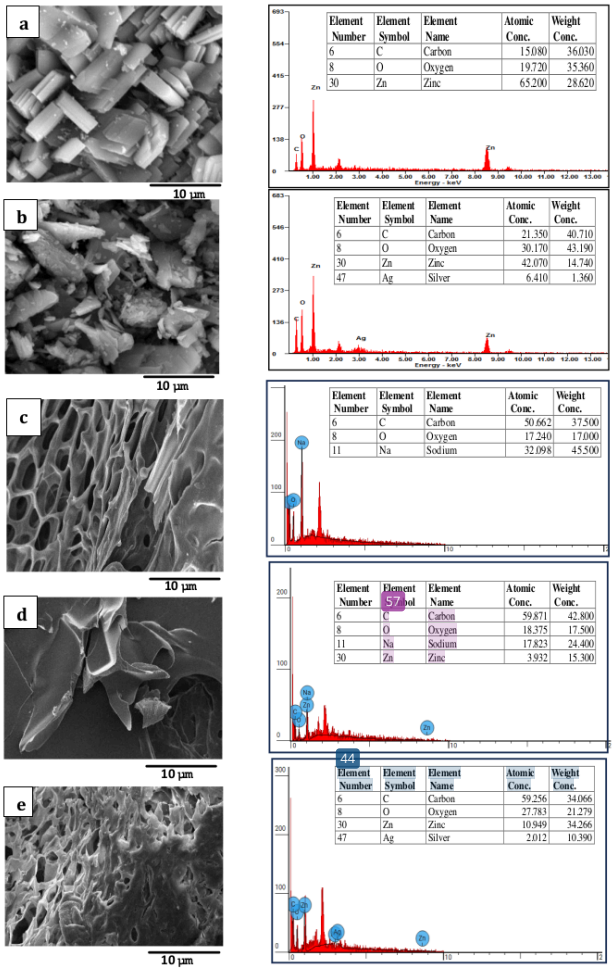

Element Number	Element Symbol	Element Name	Atomic Conc.	Weight Conc.
6	C	Carbon	15.080	36.030
8	O	Oxygen	19.720	35.360
30	Zn	Zinc	65.200	28.620

Element Number	Element Symbol	Element Name	Atomic Conc.	Weight Conc.
6	C	Carbon	21.350	40.710
8	O	Oxygen	30.170	43.190
30	Zn	Zinc	42.070	14.740
47	Ag	Silver	6.410	1.360

Element Number	Element Symbol	Element Name	Atomic Conc.	Weight Conc.
6	C	Carbon	50.662	37.500
8	O	Oxygen	17.240	17.000
11	Na	Sodium	32.098	45.500

Element Number	Element Symbol	Element Name	Atomic Conc.	Weight Conc.
6	C	Carbon	59.871	42.800
8	O	Oxygen	18.375	17.500
11	Na	Sodium	17.823	24.400
30	Zn	Zinc	3.932	15.300

Element Number	Element Symbol	Element Name	Atomic Conc.	Weight Conc.
6	C	Carbon	59.256	34.066
8	O	Oxygen	27.783	21.279
30	Zn	Zinc	10.949	34.266
47	Ag	Silver	2.012	10.390

Figure 5. SEM-EDS of (a) MOF-5; (b) Ag(20)@MOF-5; (c) Hy; (d); Hy/MOF-5 (e)Hy/Ag(20)@MOF-5.

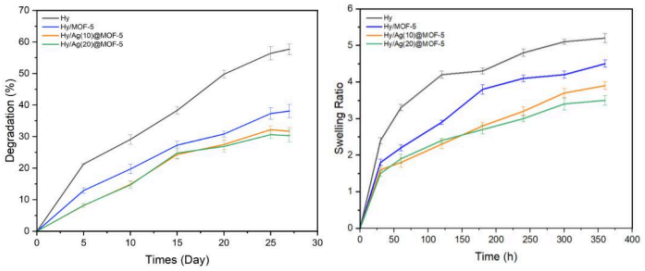

Figure 6. Swelling ratio and biodegradation profile of Hy, Hy/MOF-5, Hy/Ag(10)@MOF-5; and Hy/Ag(20)@MOF-5.

The results of EDS indicate that MOF-5 consists of the predicted elements, namely C, O, and Zn. Furthermore, Ag@MOF-5 consists of the predicted elements C, O, Zn, and Ag [37]. In addition, the Hydrogel demonstrates the predicted elements of C, O, and Na. Modification of the Hydrogel with MOF-5 shows the predicted elements of C, O, Na, and Zn. On the other hand, the Hy/Ag@MOF-5 shows the predicted elements of C, O, Zn, and Ag. These results confirm the successful production of Hydrogel modified with MOF-5 and Ag@MOF-5 [37].

The swelling and biodegradation tests in Figure 6 indicate that the addition of MOF-5 and Ag@MOF-5 in the alginate-gelatin hydrogel can reduce the swelling ratio and biodegradation percentage. In the swelling test, the Hy sample exhibited the highest swelling ratio of 5.2 after 360 minutes of immersion. In contrast, Hy/Ag(20)@MOF-5 showed the lowest swelling ratio of 3.5 after the same immersion period. The Hy/MOF-5 sample also demonstrated a decrease in swelling ratio, suggesting that MOF-5 has filled the internal pores of the hydrogel, thereby reducing the space available for water absorption and stabilizing the hydrogel matrix [19,38]. These results align with the research by Ghanbari *et al.* [39], which reported that the addition of Zn-based compounds to alginate-gelatin hydrogels can enhance the number of cross-links in the hydrogel network, thus decreasing its water absorption capacity. The incorporation of Ag@MOF-5 into the hydrogel also significantly reduced the swelling ratio. The addition of Ag@MOF-5 in the hydrogel also significantly reduces the swelling ratio, which is due to the release of Ag in the hydrogel, which increases the density of cross-linking, resulting in a denser hydrogel matrix [27]. The results of biodegradation tests also show a similar pattern with the swelling ratio. The Hy sample experienced a degradation percentage of 62.7 % on day 27, while the Hy/Ag(20)@MOF-5 sample showed a degradation percentage of 34.3 % on day 27. The Hy/MOF-5 sample also experienced a decrease in the rate of biodegradation because the integration of MOF-5 can strengthen the interactions between alginate and gelatin polymer chains, while also inhibiting the penetration of water and enzymes into the hydrogel matrix. In hydrogels modified with Ag@MOF5, a decrease in the biodegradation percentage was also observed. The increase in Ag@MOF-5 concentration also contributes to the stability of the matrix, as seen in Hy/Ag(20)@MOF-5, which is more stable compared to Hy/Ag(10)@MOF-5, indicated by the slower decrease in biodegradation percentage due to the increased number of cross-links [39].

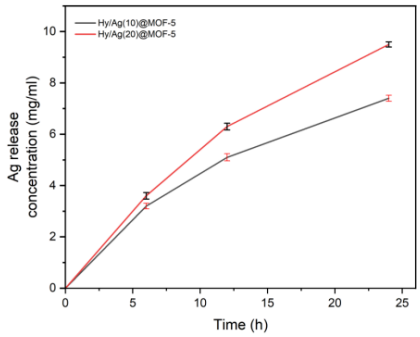

Figure 7. Cumulative release profile of Ag from Hy/Ag(10)@MOF-5 and Hy/Ag(20)@MOF-5.

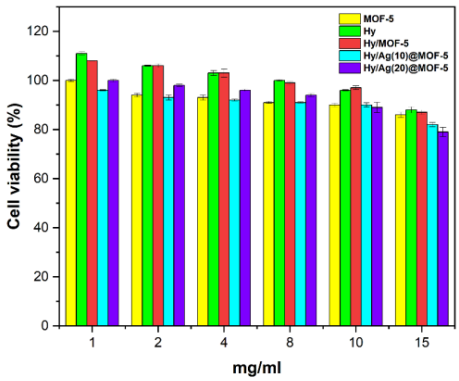

Figure 8. Cytotoxicity evaluation of Hy, MOF-5, Hy/MOF-5, Hy/Ag(10)@MOF-5, and Hy/Ag(20)@MOF-5 using the MTT assay. Data are presented as mean ± SD (n = 3).

The profile of silver ion (Ag) release from Hy/Ag(10)@MOF-5 and Hy/Ag(20)@MOF-5 samples is shown in Figure 7. Initially, the concentration of released Ag was only 3.2 µg/mL (Hy/Ag(10)@MOF-5) and 3.6 µg/mL (Hy/Ag(20)@MOF-5). The concentration of Ag gradually increased over time of immersion, reaching 7.4 µg/mL (Hy/Ag(10)@MOF-5) and 9.5 µg/mL (Hy/Ag(20)@MOF-5). In this study, the concentration of released Ag ions from the Hy/Ag(20)@MOF-5 sample tended to be higher compared to Hy/Ag(10)@MOF-5, which was attributed to the higher initial Ag content in the Hy/Ag(20)@MOF-5 sample compared to Hy/Ag(10)@MOF-5. In contrast, the release of Ag ions remained controlled. These results align with the characteristics of MOF-based hydrogels designed for the gradual release of Ag ions,

thereby supporting increased antibacterial activity and reducing toxicity risks [22].

The results of the cytotoxicity test using the MTT method are shown in Figure 8. All samples, including MOF-5, Hy, Hy/MOF-5, Hy/Ag(10)@MOF-5, and Hy/Ag(20)@MOF-5, are relatively safe for BHK-21 cells with cell viability percentages above 79%, suggesting that the integration of MOF-5 and Ag@MOF-5 in the alginate–gelatin hydrogel matrix does not cause significant toxic effects within the tested concentration range. The pure MOF-5 sample also showed high cell viability across all concentrations, confirming that the MOF-5 framework itself is biocompatible and does not exert cytotoxic effects on BHK-21 cells. In the samples Hy and Hy/MOF-5, all tested concentrations maintained high BHK-21 cell viability (>87 %), indicating no significant cytotoxic effects and categorizing them as highly biocompatible. In the samples Hy/Ag(10)@MOF-5 and Hy/Ag(20)@MOF-5, there was a slight decrease in BHK-21 cell viability with increasing concentrations, especially in Hy/Ag(20)@MOF-5, which showed a viability of 79 % at 15 mg/mL. This phenomenon corresponds to the Ag release profile, where the highest concentration of released Ag is found in Hy/Ag(20)@MOF-5, thereby increasing cellular stress. Nevertheless, the decrease is only slight and remains within the non-cytotoxic category; thus, the material can be declared safe for biomedical applications [40] and also consistent with ISO 10993-5 standards, which stipulate that cell viability of ≥70 % is categorized as non-cytotoxic. These results are in accordance with the research conducted by Amiri *et al.* [41], which reported that the modification of Ag in hydrogel composites demonstrated fibroblast cell viability of >80 %, indicating good biocompatibility.

The antibacterial activity of the samples is demonstrated by the MIC, MBC, and time-kill results. The results of the MIC and MBC in Figure 9 indicated that that the MIC results for S. aureus and E. coli followed the order: Hy > MOF-5 > Hy/MOF-5 > Hy/Ag(10)@MOF-5 > Amoxicillin > Hy/Ag(20)@MOF-5, while the MBC results showed Hy > MOF-5 > Hy/MOF-5 > Hy/Ag(10)@MOF-5 > Hy/Ag(20)@MOF-5 > Amoxicillin. The Hy sample exhibited the highest MIC and MBC (6.4 ± 0.2 mg/mL and 10.4 ± 0.2 mg/mL for S. aureus and 5.8 ± 0.2 mg/mL and 9.6 ± 0.3 mg/mL for E. coli), indicating limited antibacterial activity. The modification of MOF-5 in the hydrogel was shown to significantly reduce the MIC and MBC values, indicating the contribution of MOF-5 to enhanced antibacterial activity. These findings are consistent with the research by Maghsoudi *et al.* [19], which reports that alginate-gelatin hydrogel combined with ZIF-8 (a Zn-based MOF) can improve antibacterial activity through the release of Zn^{2+} ions from the MOF.

The modification of Ag@MOF-5 in both Hy/Ag(10)@MOF-5 and Hy/Ag(20)@MOF-5 samples also significantly enhanced antibacterial activity significantly. The Hy/Ag(20)@MOF-5 sample exhibited the best MIC and MBC values (1.2 ± 0.1 mg/mL and 2.5 ± 0.1 mg/mL for S. aureus, and 1.0 ± 0.1 mg/mL and 2.7 ± 0.2 mg/mL for E. coli) and approached the values of amoxicillin. The results indicate that the presence of Ag in the hydrogel can synergistically enhance antibacterial activity [42]. The highest antibacterial activity is shown in the sample Hy/Ag(20)@MOF-5 which exhibited a highly significant enhancement compared to Hy, further validating the role of Ag@MOF-5 in improving antibacterial efficacy. This finding is consistent with the Ag release profile in Figure 6, indicating that the sample Hy/Ag(20)@MOF-5 has a higher Ag release concentration than Hy/Ag(10)@MOF-5, thus its antibacterial effectiveness tends to be higher.

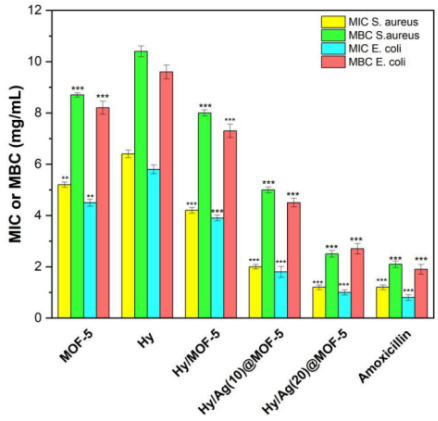

Figure 9. MIC and MBC values of Hy, MOF-5, Hy/MOF-5, Hy/Ag (10) @MOF-5, and Hy/Ag (20) @MOF-5 against *S. aureus* and *E. coli*. Data are presented as mean ± SD (n = 3). ***p < 0.001 vs Hy (one-way ANOVA followed by Tukey's post hoc test).

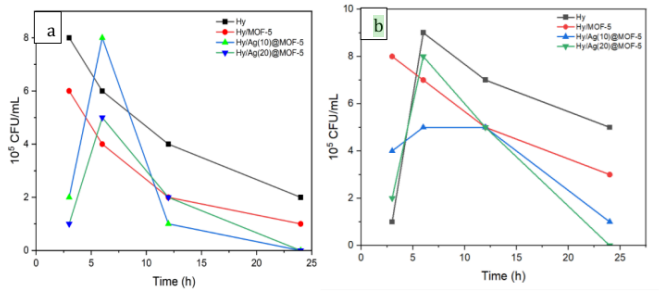

Figure 10. Time-kill assay of Hy, Hy/MOF-5, Hy/Ag(10)@MOF-5, and Hy/Ag(20)@MOF-5 against (a) *S. aureus* and (b) *E. coli.*

The results of the time-kill test (Figure 10) also show a consistent pattern with the results of the MIC and MBC tests, both against Gram-positive bacteria (*S. aureus*) and Gram-negative bacteria (*E. coli*). The control hydrogel (Hy) only exhibited a gradual decrease in the number of colonies; however, bacteria persisted for up to 24 hours at 2×10^5 CFU/mL for *S. aureus* and 5×10^5 CFU/mL for *E. coli*. The Hy/MOF-5 can accelerate bacterial death. However, bacteria were still detected at 1×10^5 CFU/mL for *S. aureus* and 3×10^5 CFU/mL for *E. coli* after 24 hours, which was attributed to the porosity of MOF-5 and the release of Zn, which has antibacterial activity [19]. In the Hy/Ag(10)-

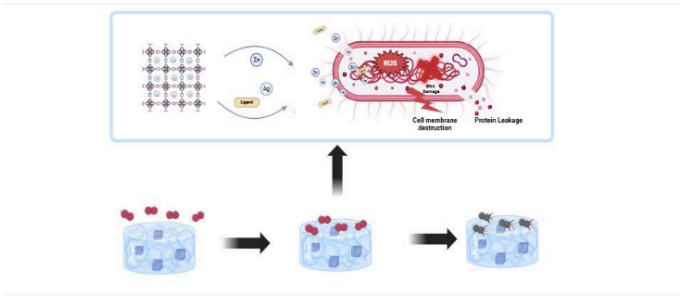

Figure 11. Schematic illustration of the antibacterial mechanism of Hy/Ag(20)@MOF-5 against *S. aureus* and *E. coli*.

@MOF-5 sample, the number of bacteria decreased dramatically, with no bacteria found after 24 hours for *S. aureus*. The most substantial antibacterial effect is demonstrated by Hy/Ag(20)@MOF-5, which is capable of killing almost the entire population within just 12 hours (2×10^3 CFU/mL for *S. aureus* and 5×10^3 CFU/mL for *E. coli*) and eliminating all bacteria within 24 hours. This indicates that the higher the concentration of Ag, the faster and more potent the bactericidal effects produced [43].

The antibacterial mechanism of the Hy/Ag(20)@MOF-5 sample is illustrated in Figure 11. In general, the alginate-gelatin hydrogel will function as a matrix that can absorb fluids, maintain moisture, and support the diffusion and release of Ag@MOF-5. The presence of MOF-5 in the sample will enhance the diffusion capacity, thereby increasing the release processes of both Zn and Ag [32,44,45]. The presence of Ag in the sample will provide a synergistic effect through the disruption of cell membranes, interference with enzymatic function and metabolism, as well as the generation of reactive oxygen species (ROS) that induce oxidative stress in bacteria [16,46–48]. In the Hy/Ag(20)@MOF-5 sample, the concentration of released Ag is higher, thus accelerating the death of both *E. coli* and *S. aureus* bacterial cells. Furthermore, the controlled release of Ag ions from the hydrogel matrix can reduce the risk of toxicity (according to cytotoxicity results) while also preventing the emergence of bacterial resistance. Thus, the synergistic effect between MOF-5 and Ag in alginate-gelatin hydrogel makes the Hy/Ag(20)@MOF-5 formulation highly promising for the development of long-term biomedical applications.

Conclusion

The Ag@MOF-5-loaded alginate–gelatin hydrogel was successfully synthesized and exhibited excellent biocompatibility and antibacterial performance. The Ag ion release profile revealed that the Hy/Ag(20)@MOF-5 sample released 7.4 µg/mL of Ag within 24 hours with a sustained release behavior. The cytotoxicity test results demonstrate cell viability >79 % across all samples, categorizing them as non-toxic and biocompatible. The best antibacterial activity was exhibited by the sample Hy/Ag(20)@MOF-5, capable of killing nearly the entire population of *S. aureus* and *E. coli* with MIC values of 1.2 ± 0.1 and 1.0 ± 0.1 mg/mL, respectively, and MBC values of 2.5 ± 0.1 and 2.7

± 0.2 mg/mL, and is capable of killing all bacteria within 24 hours. These findings suggest that the Ag@MOF-5-based alginate–gelatin hydrogel has strong potential as a biocompatible antimicrobial material for wound healing applications.

Acknowledgement

The author expresses gratitude to the Directorate of Research and Community Service (DPPM) of Indonesia for the funding support through the Fundamental Grant scheme, with contract number 128/C3/DT.05.00/PL/2025, as well as the derivative contracts numbered 099/LL7/DT.05.00/PL/2025 and 205/R/PN/VI/2025. Appreciation is also extended to the Bhakti Wiyata Foundation, Bhakti Wiyata Health Sciences Institute in Kediri, and Airlangga University for the opportunities, support, and motivation in completing this research. Special thanks are directed to all parties, both staff and students, who have contributed to the implementation of this research.

Disclosure Statement

No potential conflict of interest was reported by the authors.

ORCID

Tri Ana Mulyati: 0000-0001-8423-1209
Juni Ekowati: 0000-0002-4402-2039
Atmira Sariwati: 0000-0002-5279-9921
Lia Agustina: 0009-0001-4710-7839
Fery Eko Pujiono: 0000-0002-9859-3216

References

[1] Parveen, K., Hussain, M.A., Anwar, S., Elagib, H.M., Kausar, M.A., Comprehensive review on diabetic foot ulcers and neuropathy: Treatment, prevention and management. *World Journal of Diabetes*, **2025**, 16(3), 100329.
[2] Jais, S., Various types of wounds that diabetic patients can develop: A narrative review. *Clinical Pathology*, **2023**, 16, 2632010X231205366.
[3] Albarrak, O.S., Wound care management options for diabetic foot ulcer. *Saudi Journal of Nursing and Health Care*, **2023**, 6(11), 438–442.
[4] Mulyati, T.A., Ekowati, J., Rias, Y.A., Mu'arofah, B., Pujiono, F.E., Wardhani, S.K., Sudjatmiko, S., Harun, H.B., Identification and antibiotic susceptibility of bacterial causes from diabetic ulcers in hospital kediri, indonesia. *Journal of Chemical Health Risks*, **2024**, 14(05), 875–883.
[5] Ediati, R., Mulyati, T.A., Mukminin, A., Sulistiono, D.O., Khoiroh, N., Fansuri, H., Prasetyoko, D., Nanoporous carbon prepared with MOF-5 as a template and activated using KOH for hydrogen storage. *Jurnal Kimia Valensi*, **2020**, 6(1), 20–31.
[6] Han, D., Liu, X., Wu, S., Metal organic framework-based antibacterial agents and their underlying mechanisms. *Chemical Society Reviews*, **2022**, 51(16), 7138–7169.
[7] Hamarawf, R.F., Antibacterial, antibiofilm, and antioxidant activities of two novel metal–organic frameworks (MOFs) based on 4, 6-diamino-2-pyrimidinethiol with Zn and Co metal ions as coordination polymers. *RSC Advances*, **2024**, 14(13), 9080–9098.
[8] Mulyati, T.A., modification of Zn-metal organic framework with nano silver as an antibacterial material for diabetic ulcers (in vitro). *Research Journal of Pharmacy and Technology*, **2025**, 18(9), 10–17.
[9] Afruzi, F.H., Abdouss, M., Zare, E.N., Ghomi, E.R., Mahmoudi, S., Neisiany, R.E., Metal-organic framework-hydrogel composites as emerging platforms for enhanced wound healing applications: Material design, therapeutic strategies, and future prospects. *Coordination Chemistry Reviews*, **2025**, 524, 216330.
[10] Zou, W., Zhang, L., Lu, J., Sun, D., Recent development of metal–organic frameworks in wound healing: Current status and applications. *Chemical Engineering Journal*, **2024**, 480, 148220.
[11] Bigham, A., Islami, N., Khosravi, A., Zarepour, A., Iravani, S., Zarrabi, A., MOFs and MOF-based composites as next-generation materials for wound healing and dressings. *Small*, **2024**, 20(30), 2311903.
[12] Shakya, S., He, Y., Ren, X., Guo, T., Maharjan, A., Luo, T., Wang, T., Dhakhwa, R., Regmi, B., Li, H., Ultrafine silver nanoparticles embedded in cyclodextrin metal-organic frameworks with GRGDS functionalization to promote antibacterial and wound healing application. *Small*, **2019**, 15(27), 1901065.
[13] Xu, L., Wang, Y.-Y., Huang, J., Chen, C.-Y., Wang, Z.-X., Xie, H., Silver nanoparticles: Synthesis, medical applications and biosafety. *Theranostics*, **2020**, 10(20), 8996-9031

[14] Yao, T., Zeng, X., Tao, X., Xu, H., Recent progress of MOF-based antibacterial hydrogels. *Chemical Engineering Journal*, **2024**, 487, 150641.
[15] Zhang, M., Wang, D., Ji, N., Lee, S., Wang, G., Zheng, Y., Zhang, X., Yang, L., Qin, Z., Yang, Y., Bioinspired design of sericin/chitosan/Ag@MOF/GO hydrogels for efficiently combating resistant bacteria, rapid hemostasis, and wound healing. *Polymers*, **2021**, 13(16), 2812.
[16] Zhang, W., Ye, G., Liao, D., Chen, X., Lu, C., Nezamzadeh-Ejhieh, A., Khan, M.S., Liu, J., Pan, Y., Dai, Z., Recent advances of silver-based coordination polymers on antibacterial applications. *Molecules*, **2022**, 27(21), 7166.
[17] Vinceković, M., Jurić, S., Vlahoviček-Kahlina, K., Martinko, K., Šegota, S., Marijan, M., Krčelić, A., Svečnjak, L., Majdak, M., Nemet, I., Novel zinc/silver ions-loaded alginate/chitosan microparticles antifungal activity against botrytis cinerea. *Polymers*, **2023**, 15(22), 4359.
[18] Sheng, W., Song, Q., Su, X., Lu, Y., Bai, Y., Ji, F., Zhang, L., Yang, R., Fu, X., Sodium alginate/gelatin hydrogels loaded with adipose-derived mesenchymal stem cells promote wound healing in diabetic rats. *Journal of Cosmetic Dermatology*, **2023**, 22(5), 1670–1679.
[19] Maghsoudi, M.A.F., Asbagh, R.A., Tafti, S.M.A., Aghdam, R.M., Najjari, A., Pirayvatlou, P.S., Foroutani, L., Fazeli, A.R., Alginate-gelatin composite hydrogels loading zeolitic imidazolate framework-8 (ZIF-8) nanoparticles on gauze for burn wound healing: In vitro and in vivo studies. *International Journal of Biological Macromolecules*, **2025**, 295(139348.
[20] Hu, Y., Yang, H., Wang, R., Duan, M., Fabricating Ag@MOF-5 nanoplates by the template of MOF-5 and evaluating its antibacterial activity. *Colloids and Surfaces A: Physicochemical and Engineering Aspects*, **2021**, 626, 127093.
[21] Sacourbaravi, R., Ansari-Asl, Z., Kooti, M., Nobakht, V., Darabpour, E., Fabrication of Ag NPs/Zn-MOF nanocomposites and their application as antibacterial agents. *Journal of Inorganic and Organometallic Polymers and Materials*, **2020**, 30(11), 4615–4621.
[22] Xiong, Y., Xu, Y., Zhou, F., Hu, Y., Zhao, J., Liu, Z., Zhai, Q., Qi, S., Zhang, Z., Chen, L., Bio-functional hydrogel with antibacterial and anti-inflammatory dual properties to combat with burn wound infection. *Bioengineering & Translational Medicine*, **2023**, 8(1), e10373.
[23] Farasati Far, B., Naimi-Jamal, M.R., Jahanbakhshi, M., Hadizadeh, A., Dehghan, S., Hadizadeh, S., Enhanced antibacterial activity of porous chitosan-based hydrogels crosslinked with gelatin and metal ions. *Scientific Reports*, **2024**, 14(1), 7505.
[24] Urzedo, A.L., Goncalves, M.C., Nascimento, M.H., Lombello, C.B., Nakazato, G., Seabra, A.B., Cytotoxicity and antibacterial activity of alginate hydrogel containing nitric oxide donor and silver nanoparticles for topical applications. *ACS Biomaterials Science & Engineering*, **2020**, 6(4), 2117–2134.
[25] Li, J., Yan, Y., Chen, Y., Fang, Q., Hussain, M.I., Wang, L.-N., Flexible curcumin-loaded Zn-MOF hydrogel for long-term drug release and antibacterial activities. *International Journal of Molecular Sciences*, **2023**, 24(14), 11439.
[26] Gutiérrez, M., Martín, C., Souza, B.E., Van der Auweraer, M., Hofkens, J., Tan, J.-C., Highly luminescent silver-based MOFs: Scalable eco-friendly synthesis paving the way for photonics sensors and electroluminescent devices. *Applied Materials Today*, **2020**, 21, 100817.
[27] Diniz, F.R., Maia, R.C.A., de Andrade, L.R.M., Andrade, L.N., Vinicius Chaud, M., da Silva, C.F., Corrêa, C.B., de Albuquerque Junior, R.L.C., Pereira da Costa, L., Shin, S.R., Silver nanoparticles-composing alginate/gelatine hydrogel improves wound healing in vivo. *Nanomaterials*, **2020**, 10(2), 390.
[28] Salih, A.E., Elsherif, M., Alam, F., Chiesa, M., Butt, H., Rapid colorimetric ph-responsive gold nanocomposite hydrogels for sensing applications. *Nanomaterials*, **2022**, 12(9), 1486.
[29] Chai, Y., Zhang, Y., Wang, L., Du, Y., Wang, B., Li, N., Chen, M., Ou, L., In situ one-pot construction of MOF/hydrogel composite beads with enhanced wastewater treatment performance. *Separation and Purification Technology*, **2022**, 295, 121225.
[30] Guo, H., Zhang, Y., Zheng, Z., Lin, H., Zhang, Y., Facile one-pot fabrication of Ag@MOF(Ag) nanocomposites for highly selective detection of 2,4,6-trinitrophenol in aqueous phase. *Talanta*, **2017**, 170, 146–151.
[31] Ramli, R.H., Soon, C.F., Rus, A.Z.M., synthesis of chitosan /alginate/ silver nanoparticles hydrogel scaffold. *MATEC Web of Conferences*, **2016**, 78, 01031.
[32] Wang, J., Li, K., Yuan, H., Preparation of Ag-metal organic frameworks-loaded sodium alginate hydrogel for the treatment of periodontitis. *Scientific Reports*, **2025**, 15(1), 800.
[33] Wang, S., Xie, X., Xia, W., Cui, J., Zhang, S., Du, X., Study on the structure activity relationship of the crystal MOF-5 synthesis, thermal stability and N_2 adsorption property. *High Temperature Materials and Processes*, **2020**, 39(1), 171–177.
[34] Healy, C., Patil, K.M., Wilson, B.H., Hermanspahn, L., Harvey-Reid, N.C., Howard, B.I., Kleinjan, C., Kolien, J., Payet, F., Telfer, S.G., The thermal stability

of metal-organic frameworks. *Coordination Chemistry Reviews*, **2020**, 419, 213388.
[35] Zhu, N.-N., Liu, X.-H., Li, T., Ma, J.-G., Cheng, P., Yang, G.-M., Composite system of Ag nanoparticles and metal–organic frameworks for the capture and conversion of carbon dioxide under mild conditions. *Inorganic Chemistry*, **2017**, 56(6), 3414–3420.
[36] Wei, D., Ouyang, B., Cao, Y., Yan, L., Wu, B., Chen, P., Zhang, T., Jiang, Y., Wang, H., Coordination confined silver-organic framework for high performance electrochemical deionization. *Advanced Science*, **2024**, 11(28), 2401174.
[37] Rameesha, L., Rana, D., Nagendran, A., Fabrication and characterization of poly (vinylidene fluoride) hybrid ultrafiltration membranes with silver loaded MOF-5 for enhanced permeation, antifouling and antibiofouling performance. *Journal of Environmental Chemical Engineering*, **2023**, 11(3), 109888.
[38] Yu, J., Huang, X., Wu, F., Feng, S., Cheng, R., Xu, J., Cui, T., Li, J., 3D-printed hydrogel scaffolds loaded with flavanone@ ZIF-8 nanoparticles for promoting bacteria-infected wound healing. *Gels*, **2024**, 10(12), 835.
[39] Ghanbari, M., Sadjadinia, A., Zahmatkesh, N., Mohandes, F., Dolatyar, B., Zeynali, B., Salavati-Niasari, M., Synthesis and investigation of physicochemical properties of alginate dialdehyde/gelatin/ZnO nanocomposites as injectable hydrogels. *Polymer Testing*, **2022**, 110, 107562.
[40] Ghasemi, M., Turnbull, T., Sebastian, S., Kempson, I., The MTT assay: Utility, limitations, pitfalls, and interpretation in bulk and single-cell analysis. *International Journal of Molecular Sciences*, **2021**, 22(23), 12827.
[41] Amiri, N., Ghaffari, S., Hassanpour, I., Chae, T., Jalili, R., Kilani, R.T., Ko, F., Ghahary, A., Lange, D., Antibacterial thermosensitive silver–hydrogel nanocomposite improves wound healing. *Gels*, **2023**, 9(7), 542.
[42] Zhou, K., Zhang, Z., Xue, J., Shang, J., Ding, D., Zhang, W., Liu, Z., Yan, F., Cheng, N., Hybrid Ag nanoparticles/polyoxometalate-polydopamine nano-flowers loaded chitosan/gelatin hydrogel scaffolds with synergistic photothermal/chemodynamic/Ag^+ anti-bacterial action for accelerated wound healing. *International Journal of Biological Macromolecules*, **2022**, 221, 135–148.
[43] Girma, A., Alamnie, G., Bekele, T., Mebratie, G., Mekuye, B., Abera, B., Workineh, D., Tabor, A., Jufar, D., Green-synthesised silver nanoparticles: Antibacterial activity and alternative mechanisms of action to combat multidrug-resistant bacterial pathogens: A systematic literature review. *Green Chemistry Letters and Reviews*, **2024**, 17(1), 2412601.
[44] Zhao, X., Qiu, H., Shao, Y., Wang, P., Yu, S., Li, H., Zhou, Y., Zhou, Z., Ma, L., Tan, C., Silver nanoparticle-modified 2D MOF nanosheets for photothermally enhanced silver ion release antibacterial treatment. *Acta physico-chimica Sinica*, **2023**, 39(7), 221104.
[45] Aghdam, A.H., Javanbakht, S., Mohammadi, R., In-situ anchoring an Ag-based metal-organic framework onto carboxymethylcellulose hydrogel film: A potential bio-platform for antibiotic-free wound dressing. *Carbohydrate Polymer Technologies and Applications*, **2025**, 11, 100943.
[46] Du, J., Hou, J., Liu, S., Wu, X., Hu, L., Xu, W., Zhuo, S., Curcumin-loaded silver-based metal–organic frameworks: Efficient antibacterial and antioxidant properties against *Escherichia coli* and *Staphylococcus aureus* for promoting infected wound healing. *ACS Applied Bio Materials*, **2025**, 8(5), 4140–4152.
[47] Meng, X., Sun, S., Gong, C., Yang, J., Yang, Z., Zhang, X., Dong, H., Ag-doped metal–organic frameworks' heterostructure for sonodynamic therapy of deep-seated cancer and bacterial infection. *ACS Nano*, **2022**, 17(2), 1174–1186.
[48] Tu, C., Lu, H., Zhou, T., Zhang, W., Deng, L., Cao, W., Yang, Z., Wang, Z., Wu, X., Ding, J., Promoting the healing of infected diabetic wound by an anti-bacterial and nano-enzyme-containing hydrogel with inflammation-suppressing, ROS-scavenging, oxygen and nitric oxide-generating properties. *Biomaterials*, **2022**, 286, 121597.

HOW TO CITE THIS ARTICLE

T.A. Mulyati, J. Ekowati, A. Sariwati, L. Agustina, F.E. Pujiono. Cytotoxicity and Antibacterial Activity of Ag@MOF-5 Loaded Alginate–Gelatin Hydrogel as a Promising Antimicrobial Biomaterial. *Adv. J. Chem. A*, 2026, 9(4), 577-593.

DOI: 10.48309/AJCA.2026.547525.1928
URL: https://www.ajchem-a.com/article_233205.html

Cytotoxicity and Antibacterial Activity of Ag@MOF-5 Loaded Alginate–Gelatin Hydrogel as a Promising Antimicrobial Biomaterial

ORIGINALITY REPORT

18%	13%	14%	%
SIMILARITY INDEX	INTERNET SOURCES	PUBLICATIONS	STUDENT PAPERS

PRIMARY SOURCES

1	www.mdpi.com Internet Source	2%
2	Dharmendra Kumar Yadav, Vellaichamy Ganesan, Frank Marken, Rupali Gupta, Piyush Kumar Sonkar. "Metal@MOF Materials in Electroanalysis: Silver-Enhanced Oxidation Reactivity Towards Nitrophenols Adsorbed into a Zinc Metal Organic Framework—Ag@MOF-5(Zn)", Electrochimica Acta, 2016 Publication	1%
3	Ryhan Abdullah Rather, Zeba N. Siddiqui. " Silver phosphate supported on metal–organic framework (Ag PO @MOF-5) as a novel heterogeneous catalyst for green synthesis of indenoquinolinediones ", Applied Organometallic Chemistry, 2019 Publication	1%
4	iptek.its.ac.id Internet Source	1%
5	digitallibrary.bishopmoorecollege.ac.in Internet Source	1%
6	www.researchgate.net Internet Source	<1%
7	Irvan Dahlan, Christopher Chiedozie Obi, Noor Suhaila Razaman, Harahsheh Yazeed Ahmad Hasan. "Adsorptive Decolorization of	<1%

Brilliant Green Dye in Aqueous Media Using Various Modified MOF-5 Adsorbents", Groundwater for Sustainable Development, 2024
Publication

8	pubs.rsc.org Internet Source	<1 %
9	Jie Wu, Leyi Liu, Runze Li, Kuangwu Pan et al. "MIL-53(Fe)-Glucose self-assembled complex for enhanced angiogenesis and endothelial tip cell activation", Journal of Nanobiotechnology, 2025 Publication	<1 %
10	repository.ubaya.ac.id Internet Source	<1 %
11	www.science.gov Internet Source	<1 %
12	repositorio.uchile.cl Internet Source	<1 %
13	innovareacademics.in Internet Source	<1 %
14	tuprints.ulb.tu-darmstadt.de Internet Source	<1 %
15	www.engineering.org.cn Internet Source	<1 %
16	Hadhemi Ben Attia, Mohammed S.M. Abdelbaky, Alberto Martín Santa Daría, Santiago García-Granda, Mohamed Dammak. "Dual-Function Copper(II) Complex: Low Band Gap Solar Absorber with High Dielectric Constant for Advanced Optoelectronic Applications", Optical Materials, 2025 Publication	<1 %

www.thno.org

17	Internet Source	<1 %
18	www2.mdpi.com Internet Source	<1 %
19	Rui Zhang, Zhe Xu, Meiqi Gu, Penghui Xiang, Yifei Li, Fei Xin, Yuying Cai, Yuchen Xie, Xu Yu, Li He, Chengla Yi. "Construction of Silver-Ion Functionalized Metal-Organic Framework with levofloxacin Nanocomposites and Its Multi-Mechanism Synergistic Antibacterial Performance", Colloids and Surfaces A: Physicochemical and Engineering Aspects, 2025 Publication	<1 %
20	Shuying Chen, Yahui Xiong, Fan Yang, Yanke Hu et al. "Approaches to scarless burn wound healing: application of 3D printed skin substitutes with dual properties of anti-infection and balancing wound hydration levels", eBioMedicine, 2024 Publication	<1 %
21	Xiao, C.. "Synthesis and properties of degradable poly(vinyl alcohol) hydrogel", Polymer Degradation and Stability, 2003 Publication	<1 %
22	learning-gate.com Internet Source	<1 %
23	www.ijese.net Internet Source	<1 %
24	Leonarda Vukonic, Nádia E. Santos, Christoph Bauer, Felix Groß et al. "Nano-Ru-HKUST-1 enhanced PVA hydrogels: Laying the foundation for MOF-based cartilage tissue scaffolds", Materials Today Chemistry, 2026 Publication	<1 %

25	Qunling Fang, Jing Wang, Qingshan Xiong, Yunqi Xu, Guangjin Yu, Ailing Hui, Ken Cham-Fai Leung, Shouhu Xuan. " Anisotropic α-Fe O /AgAu/Polydopamine Nanostructures for Photothermally Enhanced Antibacterial Applications ", ACS Applied Nano Materials, 2023 Publication	<1 %
26	www.rsc.org Internet Source	<1 %
27	Aladpoosh, Razieh, and Majid Montazer. "Nano-photo active cellulosic fabric through in situ phytosynthesis of star-like Ag/ZnO nanocomposites: Investigation and optimization of attributes associated with photocatalytic activity", Carbohydrate Polymers, 2016. Publication	<1 %
28	Amin Hashemi Aghdam, Siamak Javanbakht, Reza Mohammadi. "In-situ anchoring an Ag-based metal-organic framework onto carboxymethylcellulose hydrogel film: A potential bio-platform for antibiotic-free wound dressing", Carbohydrate Polymer Technologies and Applications, 2025 Publication	<1 %
29	Ivan Ristić, Ljubiša Nikolić, Suzana Cakić, Vesna Nikolić, Jelena Tanasić, Jelena Zvezdanović, Marija Krstić. "Eco-Friendly Microwave Synthesis of Sodium Alginate-Chitosan Hydrogels for Effective Curcumin Delivery and Controlled Release", Gels, 2024 Publication	<1 %
30	Nikolina A. Travlou, Manuel Algarra, Cristina Alcoholado, Manuel Cifuentes-Rueda et al. "Carbon Quantum Dot Surface-Chemistry-	<1 %

	Dependent Ag Release Governs the High Antibacterial Activity of Ag-Metal–Organic Framework Composites", ACS Applied Bio Materials, 2018 Publication	
31	dramp.cpu-bioinfor.org Internet Source	<1 %
32	www.coudert.name Internet Source	<1 %
33	www.ijeat.org Internet Source	<1 %
34	bionaturajournal.com Internet Source	<1 %
35	etheses.whiterose.ac.uk Internet Source	<1 %
36	journal.uinjkt.ac.id Internet Source	<1 %
37	www.benchchem.com Internet Source	<1 %
38	www.nrcresearchpress.com Internet Source	<1 %
39	Georgiana Dolete, Cornelia-Ioana Ilie, Cristina Chircov, Bogdan Purcăreanu et al. "Synergistic Antimicrobial Activity of Magnetite and Vancomycin-Loaded Mesoporous Silica Embedded in Alginate Films", Gels, 2023 Publication	<1 %
40	public-pages-files-2025.frontiersin.org Internet Source	<1 %
41	www.biorxiv.org Internet Source	<1 %
42	www.hindawi.com Internet Source	<1 %

43	ehjournal.biomedcentral.com Internet Source	<1 %
44	etheses.uin-malang.ac.id Internet Source	<1 %
45	www.osti.gov Internet Source	<1 %
46	Fifi Gus Dwiyanti, Irsyad Kamal, Rahadian Pratama, Dhika Syaputra et al. "Whole genome sequencing of Neolamarckia macrophylla (Roxb.) Bosser and Neolamarckia cadamba (Roxb.) Bosser from Indonesia: a vital resource for completing chloroplast genomes and mining microsatellite markers", Frontiers in Plant Science, 2025 Publication	<1 %
47	Tao You, Jian Chen, Yuesheng Zhu, Na Shan, Zejun Gao, Yao Shen, Yaojun Yu. "Novel preparation of pH-responsive hydrogel with chitosan-based microbeads for targeted oral delivery of bevacizumab to enhanced apoptosis in azoxymethane-induced colorectal cancer: cellular and in vivo mice models", Drug Delivery and Translational Research, 2025 Publication	<1 %
48	eprints.ucm.es Internet Source	<1 %
49	gfzpublic.gfz.de Internet Source	<1 %
50	mdpi-res.com Internet Source	<1 %
51	opus.lib.uts.edu.au Internet Source	<1 %
	research.chalmers.se	

52	Internet Source	<1 %
53	www.jstage.jst.go.jp Internet Source	<1 %
54	Antanas Straksys, Adei Abouhagger, Monika Kirsnytė-Šniokė, Tatjana Kavleiskaja, Arunas Stirke, Wanessa C. M. A. Melo. "Development and Characterization of a Gelatin-Based Photoactive Hydrogel for Biomedical Application", Journal of Functional Biomaterials, 2025 Publication	<1 %
55	Jin Mu, Wenhui Xu, Zhenzhen Huang, Qiong Jia. "Encapsulating copper nanoclusters in 3D metal-organic frameworks to boost fluorescence for bio-enzyme sensing, inhibitor screening, and light-emitting diode fabrication", Microchemical Journal, 2023 Publication	<1 %
56	Mengke Zhan, Danyang Zhou, Lijing Lei, Jinhua Zhu, Md. Zaved H. Khan, Xiuhua Liu, Fanyi Ma. "Glycyrrhizic acid and glycyrrhetinic acid loaded cyclodextrin MOFs with enhanced antibacterial and anti-inflammatory effects for accelerating diabetic wound healing", Colloids and Surfaces B: Biointerfaces, 2025 Publication	<1 %
57	R Docampo. "The acidocalcisome", Molecular and Biochemical Parasitology, 2001 Publication	<1 %
58	Sabahat Sarfaraz, Midhat Batool Zaidi, Abdul Jabbar, Maria Khalid et al. "Enhancement of wound healing via conjugated polymeric serum of curcumin, silver, and metal-organic	<1 %

	frameworks", Journal of Drug Delivery Science and Technology, 2025 Publication	
59	Siamak Javanbakht, Reza Mohammadi. "Double cross-linking oxidized sodium alginate with Ag-based metal-organic framework and borax as an antibacterial spray-filming hydrogel for bacterial barrier", Carbohydrate Polymer Technologies and Applications, 2024 Publication	<1 %
60	Yuchen Hu, Junchao Zhou, Yuhang Gao, Ying Fan, Ban Chen, Jiangtao Su, Hong Li. "Multifunctional nanocomposite hydrogels: an effective approach to promote diabetic wound healing", Biomedical Materials, 2025 Publication	<1 %
61	Zubair Hashmi, Ibrahim Maina Idriss, Femiana Gapsari, Norazanita Samsuddin, Muhammad Roil Bilad. "The Role of Nanomaterials in Enhancing Membrane-Based Treatment for Emerging Contaminants: A Review", Sustainable Chemistry for Climate Action, 2025 Publication	<1 %
62	gmpc-akademie.de Internet Source	<1 %
63	patents.google.com Internet Source	<1 %
64	pdm-mipa.ugm.ac.id Internet Source	<1 %
65	pubs.acs.org Internet Source	<1 %
66	www.paspk.org Internet Source	<1 %

67	M.T. Khulood, U.S. Jijith, P.P. Naseef, Sirajudheen M. Kallungal, V.S. Geetha, K. Pramod. "Advances in metal-organic framework-based drug delivery systems", International Journal of Pharmaceutics, 2025 Publication	<1 %
68	Bhakti Pawar, Shivam Otavi, Amrita Singh, Simranjeet Kaur, Rakesh K. Tekade. "On-demand Opto-Laser activatable nanoSilver ThermoGel for treatment of full-thickness diabetic wound in a mouse model", Biomaterials Advances, 2024 Publication	<1 %
69	Kibrya Farooq, Vijay Kumar, Vishal Sharma, Madhulika Bhagat, Vaneet Kumar, Kashma Sharma. "Synthesis, optimization, and multifunctional evaluation of amla-based novel biodegradable hydrogel", Polymer Bulletin, 2024 Publication	<1 %
70	Lihan Cai, Jianjun Du, Fuping Han, Tiancong Shi, Han Zhang, Yang Lu, Saran Long, Wen Sun, Jiangli Fan, Xiaojun Peng. "Piezoelectric Metal–Organic Frameworks Based Sonosensitizer for Enhanced Nanozyme Catalytic and Sonodynamic Therapies", ACS Nano, 2023 Publication	<1 %
71	Mohammed Sanad Alhussaini, AbdulRahman Abdulla Ibrahim Alyahya, Abdullah Abdulrahman Al-Ghanayem. "Alginate-derived antibacterial and antifungal agents: A review of applications and advancements (2019–2025)", International Journal of Biological Macromolecules, 2025 Publication	<1 %

72	Siyang Deng, Huan Liu, Chunhui Zhang, Xinting Yang, Christophe Blecker. "LMOF serve as food preservative nanosensor for sensitive detection of nitrite in meat products", LWT, 2022 Publication	<1 %
73	Sumeyya Deniz Aybek, Mucahit Secme, Hasan Ilhan, Leyla Acik, Suheyla Pinar Celik, Gonca Gulbay. "Multifaceted Applications of Zerumbone-Loaded Metal–Organic Framework-5: Anticancer, Antibacterial, Antifungal, DNA-Binding, and Free Radical Scavenging Potentials", Molecules, 2025 Publication	<1 %

Exclude quotes	On	Exclude matches	Off
Exclude bibliography	On		

Cytotoxicity and Antibacterial Activity of Ag@MOF-5 Loaded Alginate–Gelatin Hydrogel as a Promising Antimicrobial Biomaterial

GRADEMARK REPORT

FINAL GRADE

/100

GENERAL COMMENTS

PAGE 1

PAGE 2

PAGE 3

PAGE 4

PAGE 5

PAGE 6

PAGE 7

PAGE 8

PAGE 9

PAGE 10

PAGE 11

PAGE 12

PAGE 13

PAGE 14

PAGE 15

PAGE 16

PAGE 17